An in-depth look at the Fe rich liquidus in the Fe-FeS system from 1 Bar to 14 GPa

Antonio Buono, Dave Walker
Columbia University
Presenter: Antonio Buono

Abstract

Sulfur has long been indicated as a component in the iron rich cores of planetary bodies. As such it is important to understand the change in the position and shape of the Fe-FeS liquidus through pressure in order to constrain core conditions. Complicating attempts to do this is the presence of an interesting pathology that appears in the Fe rich side of the 1 bar (10-4 GPa) Fe-FeS liquidus presented by Hansen and Anderko (1958). Negative curvature suggests the presence of a metastable solvus near the liquidus, whichwhich seems to be the result of non-ideal liquid solution behavior. Brett and Bell (1969) showed that at 3 GPa this pathology appeared to relax and the liquid solution became more ideal. In order to more fully understand this relaxation we investigated the system at 6 GPa and modeled the liquid solution through 10 GPa using an asymmetric Margules formulation and found that this relaxation indicates a continued shrinking of the solvus. By 14 GPa Chen (2007) shows that the liquidus re-kinks and thus reverts back to a structure similar to its shape at 1 bar. Our model breaks down when the liquidus re-kinks at 14 GPa, requiring us to vary the WH term to model the values accurately.

The newly determined liquidus at 6 GPa, in conjunction with the previously determined 1 bar, 3 GPa and 10 GPa liquidi for the Fe-FeS system, shows an increase in the temperature separation of the crest of the solvus and the liquidus with increasing pressure. The solvus crest grows higher in temperature with pressure and becomes more asymmetric, leaning towards the Fe-rich end-member. Because the solvus does not rise in temperature as quickly as the liquidus does, the liquidus is less kinked with increasing pressure. The 1 bar, 3 GPa, 6 GPa, and 10 GPa all cross at 1642±20K and FeS36±1, providing a compositional location that is pressure independent through 10GPa. The 14 GPa line deviates sharply from the lower pressure trends indicating that the solvus is re-stabilized and grows with respect to the 14 GPa liquidus.

Summary

(1) From 1 bar through 6 GPa the eutectic remains constant in temperature and becomes more Fe rich in composition. After 6 GPa the eutectic no longer appears to be constant in temperature.

(2) As pressure increases from 1 bar to 14 GPa the melting temperature of Fe increases.

(3) Float experiments show that the accepted values for high pressure melting of Fe are low.

(4) As pressure increases from 1 bar to 10 GPa the liquidus relaxes, then by 14 GPa suddenly re-kinks.

(5) The 3, 6, and 10 GPa liquidi cross the 1 bar liquidus at a fairly constant temperature of 1630 K and with a deviation of no more than 3 wt% Fe.

(6) The straightening out of the liquidus from 1 bar to 10 GPa appears to be associated with a negative excess volume.

(7) The shape of the liquidus from 1 bar to 10 GPa can be modeled accurately with an asymmetric form of the Margules equations. By 14 GPa this is no longer the case.

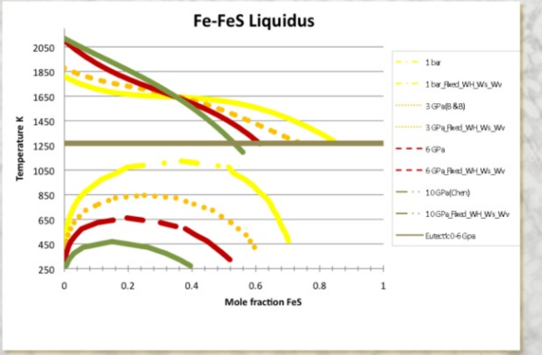

Additional Information

The image above shows the 1bar, 3 GPa, 6 GPa, and 10 GPa liquidi and the solvi associated with them as derived using the W values from the table below.

The first 5 images on the left use the WG values listed in the table below to calculate a liquidus at each pressure of interest.

The W values reported below are applied using the relation WG=WH-TWS+PWV. Using a single WH, WS, and WV value for pressures from 1bar to 10 GPa results in reasonable liquidi up to 10 GPa. By 14 GPa this is no longer the case.

The last figure shows the best fit lines to the experimental data through pressure. The 1-10 GPa liquidi pass through a single P,T point and appear to become more ideal with increasing pressure. By 14 GPa none of these relations appear to hold.

WH1(FeS) KJ/Mole	21.56	WS1(FeS) KJ/Mole K	0.00062	WV1(FeS) KJ/Mole GPa	-2.15
WH2(Fe) KJ/Mole	-22.698	WS2(Fe) KJ/Mole K	-0.032	WV2(Fe) KJ/Mole GPa	-2.090

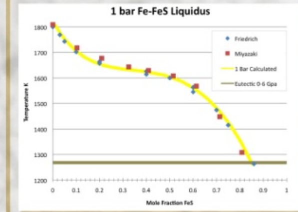

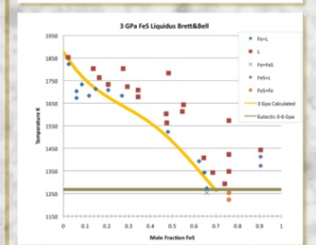

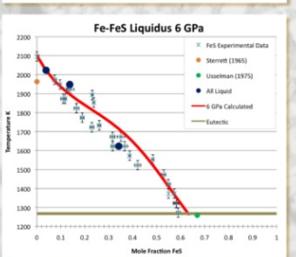

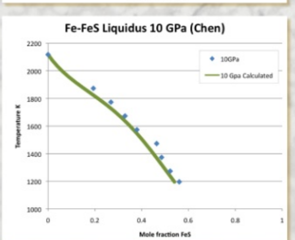

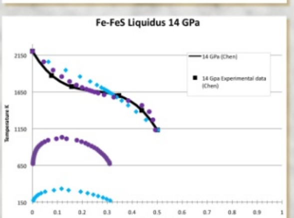

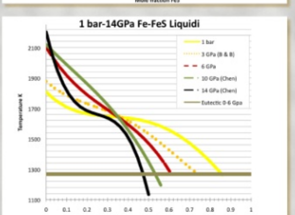

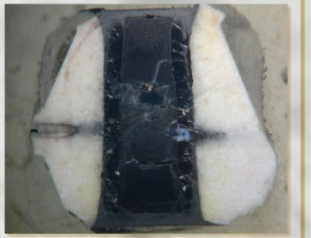

Above is a cross sectional view of a Standard Multi-anvil charge. Below is an image of the change, the upper portion (colder) is the metallic part, the lower portion (hotter) is the liquid section. Both images are oriented so that the thermocouple is down.

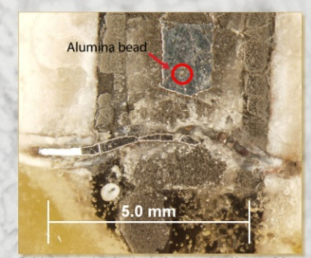

Both images are oriented so that the thermocouple and bottom of the capsule is down. The image above (TT_707) shows the alumina ball near the base of the capsule, the Fe below the alumina ball was placed there to insulate the ball from the capsule walls. The lack of motion indicates that no melting occurred by 2073±25 K. The image below (TT_706) shows the alumina ball 3/4th of the way to the top indicating melting occurred by 2123±25 K.

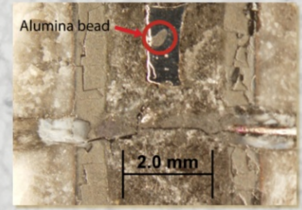

References Cited

Anderson, O.L. and Isaak, D.G., 2000, Calculated melting curves for phases of iron: American Mineralogist, v. 85, p. 376-385.

Barin, I., 1989, Thermochemical Data of Pure Substances: Part I: Weinheim (Federal Republic of Germany), VCH, p. 536.

Bassett, W.A. and Weathers, M.S., 1990, Stability of the Body-Centered Cubic Phase of Iron: A Thermodynamic Analysis: Journal of Geophysical Research, v. 95, p. 21709-21711.

Boehler, R., von Bargen, N., and Chopelas, A., 1990, Melting, Thermal Expansion, and Phase Transitions of Iron and High Pressure: Journal of Geophysical Research, v. 95, p. 21731-21736.

Brett, R. and Bell, P.M., 1969, Melting relations in the Fe-rich portion of the system Fe-FeS at 30 kb pressure: Earth and Planetary Science Letters, v. 6, p. 479-482.

B. Chen, J. Li, and S.A. Hauck, II, Non-ideal liquidus curve in the Fe-S system and Mercury's snowing core, Geophys. Res. Lett. 35 (2008), p. L07201.

Fei, Y., Bertka, C.M., and Finger, L.W., 1997, High Pressure Iron-Sulfur Compound, Fe_3S_2, and Melting Relations in the Fe-FeS System: Science, v. 275, p. 1621-1623.

Friedrich, K., 1910, Metallurgie p. 257-261.

Hansen, M. and Anderko, K., 1958, Constitution of the binary alloys: New York, McGraw-Hill Book Co.

Iglesias, R. and Palacios, S.L., 2007, Ab initio studies on the magnetic phase stability of iron: Acta Materialia, v. 55, p. 5123-5127.

Kress, V., 1997, Thermochemistry of sulfide liquids I. the system O-S-Fe at 1 bar: Contrib Mineral Petrol, v. 127, p. 176-186.

Majewski, E. and Walker, D., 1998, S diffusivity in Fe-Ni-S-P melts: Earth and Planetary Science Letters, v. 160, p. 823-830.

Miyazaki, K., 1928, The Equilibrium Diagram of the Iron and Iron Sulphide System: Science Reports of the Tohoku Imperial University, v. 17, p. 877-881.

Muller, M., Erhart, P., and Albe, K., 2007, Analytic bond-order potential for bcc and fcc iron - comparison with established embedded-atom method potentials: Journal of Physics-Condensed Matter, v. 19.

Ryzhenko, B. and Kennedy, G.C., 1973, The Effect of Pressure on the Eutectic in the System Fe-FeS: American Journal of Science, v. 273, p. 803-810.

Sterrett, K.F., Klement, W.Jr., and Kennedy, G.C., 1965, Effect of pressure on the melting of iron: Journal of Geophysical Research, v. 70, p. 1979-1984.

Strong, H.M., Tuft, R.E., and Hanneman, R.E., 1973, Iron Fusion Curve and Gamma-Delta-l Triple Point: Metallurgical Transactions, v. 4, p. 2657-2661.

Thompson J.B., Jr., 1967, Thermodynamic Properties of Simple Solutions: Advances in Geochemistry, v. 2, p. 340-361.

Thompson J.B., Jr. and Waldbaum, D.R., 1969, Analysis of the two-phase region halite-sylvite in the system NaCl-KCl: Geochimica et Cosmochimica Acta, v. 33, p. 671-690.

Usselman, T.M., 1975, Experimental Approach to the state of the core: Part I. The liquidus relations of the Fe-rich portion of the Fe-Ni-S system from 30 to 100 Kb: American Journal of Science, v. 275, p. 278-290.

Walker, D., 1999, Core Participation in Mantle Geochemistry: Geochimica et Cosmochimica Acta, v. 64, p. 2897-2911.

Walker, D., Verma, P.K., Cranswick, L.M.D., Clark, S.M., Jones, R.L., and Buhre, S., 2005, Halite-sylvite thermoconsolution: American Mineralogist, v. 90, p. 229-239.